Role of template layer on microstructure, phase formation and polarization behavior of ferroelectric relaxor thin films

R. Ranjith, Ayan Roy Chaudhuri, S. B. Krupanidhi, and P. Victor

Citation: Journal of Applied Physics **101**, 104111 (2007); doi: 10.1063/1.2733656
View online: http://dx.doi.org/10.1063/1.2733656
View Table of Contents: http://scitation.aip.org/content/aip/journal/jap/101/10?ver=pdfcov
Published by the AIP Publishing

Role of template layer on microstructure, phase formation and polarization behavior of ferroelectric relaxor thin films

R. Ranjith,[a] Ayan Roy Chaudhuri, and S. B. Krupanidhi
Materials Research Centre, Indian Institute of Science, Bangalore 560 012 India

P. Victor
Materials Science and Engineering, Rennsalaer Polytechnic Institute, Troy, New York 12180

(Received 11 December 2006; accepted 20 March 2007; published online 25 May 2007)

$(1-x)Pb(Mg_{1/3}Nb_{2/3})O_3-(x)PbTiO_3$ (PMNPT) a relaxor ferroelectric has gained attention due to its interesting physical properties both in the bulk and thin film forms from a technological and fundamental point of view. The PMNPT solid solution at the morphotropic phase boundary composition has superior properties and is potentially used as an electrostrictive actuator, sensor, and in MEMS applications. Deposition of phase pure PMNPT thin films on bare platinized silicon wafers has been an impossible task so far. In this study the role of the LSCO template on the phase formation and the influence of platinum surface on the same have been studied. It was observed that formation of hillocks in Pt coated silicon wafers is associated with an ATG type of instability while roughening through strain relaxation. The hillocks formation was observed only on the troughs of the strain waves on the surface of Pt. The nucleation and growth of the PMNPT films were analyzed using AFM studies and the nucleation nucleates only at the tips of the hillocks and grows along the same direction with a new nucleus adjacent to the first one. A wavy pattern of PMNPT nuclei was observed and later the lateral growth of the islands takes place to cover the surface and minimizes the roughness to 2 nm. Hence, a template layer with a minimum of 40 nm is required to have a complete coverage with a roughness of less than 2 nm. The chemical states of the PMNPT films grown with and without the template layer were analyzed using x-ray photoelectron spectrum. The XPS spectrum of PMNPT deposited on a Pt surface exhibited a reduced oxidation state of niobium ions and a metallic state of Pb at the initial stage of the growth, which effectively destabilizes the perovskite phase of PMNPT in which the charge states and the ordering of Nb and Mg are more crucial to have a stable perovskite structure. © *2007 American Institute of Physics*.
[DOI: 10.1063/1.2733656]

I. INTRODUCTION

Relaxor ferroelectrics (FE) have attracted much attention from both the fundamental and applications point of view over a few decades.[1–3] They exhibit a variety of physical phenomena and excellent electromechanical properties both in the form of bulk ceramics and thin film form.[4] A $(B'B'')O_3$ type of distorted perovskites is known to exhibit relaxor behavior due to the presence of local disorder in the structural ordering of the *B*-site cation, in our case the $B'a+2$ and $B''a+5$ cation. $Pb(Mg_{1/3}Nb_{2/3})O_3$ shortly known as PMN and its solid solution with $PbTiO_3$ known as PMNPT are well-known members of the relaxor FE and have been studied extensively. Apart from their interesting physical properties, these relaxors are known to have a complicated crystallographic structural ordering. The structural aspects of these class of relaxor FE has been studied extensively by XRD,[5,6] TEM,[7–9] neutron diffraction studies,[10,11] and NMR.[12] PMN is known to exhibit a cubic symmetry through the temperatures above and below the FE transition temperature when observed under a normal powder XRD studies. Under extensive structural investigation under high resolution XRD, TEM, neutron, and NMR the existence of a short range local symmetry, different from the global symmetry of the system, was confirmed.

The local polar region was known to have a 1:1 ordering of Mg^{2+} and Nb^{5+} cations over the alternate lattice planes along the ⟨111⟩ direction giving rise to a rhombohedral symmetry. Various structural models were proposed, such as the space charge model[13] and random site model,[14] to explain the structural aspects of these distorted perovskite systems. The random site model was successful over proving the analogy of the polar regions with the ferroelectric domain structure through observing the growth of these nano regions on thermal treatments. A 1:1 ordering of the Mg^{2+} and Nb^{5+} ions over the alternate lattice planes in the nano polar regions over a matrix of Nb^{5+} ions is a most widely accepted structural ordering of PMN and other iso-structural systems of the same family. The polar regions were observed to have a translation symmetry and exhibited a size distribution of 3 – 10 nm. The chemical heterogeneity and the polarization fluctuation due to the existence of local polar regions are responsible for the relaxor behavior of the distorted $A(B'B'')O_3$ type of structure.[1,2]

Though PMN is known to exhibit interesting physical properties, the ferroelectric to super paraelectric transition temperature is below room temperature and limits its usage

[a]Electronic mail: vtcranjith@gmail.com

in practical applications.[2] Hence, a solid solution of PMN with PT is used which effectively increases the ferroelectric to paraelectric transition temperatures depending on the composition of PT.[15] A combination of 0.67 at. % of PMN with 0.33 at. % of PT is known as the morphotropic phase boundary that separates the rhombohedral and tetragonal phase of PMNPT. Below 0.33 at. % of PT, PMNPT exhibits a relaxorlike behavior with a rhombohedral symmetry and a transition temperature of around 150 °C and above which it exhibits a normal FE type of behavior with a tetragonal symmetry. The structural aspects of the PMN are still retained until the composition of PT exceeds 0.33 at. % as explained above.[15]

Fabrication of these systems as thin films has been the interest for realization of the physical properties of these relaxor materials in miniaturization of devices for MEMS, electrostrictive actuator, and sensor applications.[4] Platinum coated silicon substrates have been a potential candidate to deposit various FE thin films in which, the platinum acts as a bottom electrode, as well as the nucleating surface of the thin film and hence allows the characterization of a FE thin film in a metal-insulator-metal (MIM) configuration.[16]

Growth of a phase pure pyrochlore free PMNPT thin film over bare platinum surfaces has not been realized, and hence $La_{0.5}Sr_{0.5}CoO_3$ (LSCO) an electronically conducting oxide acting as a template layer was used to assist the growth of PMNPT over platinum substrates.[17] The role of the LSCO template layer over the phase formation of PMNPT and the cause of instability of the PMNPT perovskite phase on bare platinum surfaces remains ambiguous. The substrate surface and their modifications play a crucial role in deciding the phase formation and the microstructure of the thin film fabricated.[18] Platinum coated over TiO_2/Ti a buffer layer over silicon wafer with native SiO_2 is the configuration of the commercially available platinized silicon wafers (Inostek, Korea). Thus ,obtained or fabricated platinum thin films are known to undergo several surface modifications and roughening processes when subjected to various deposition conditions.[19,20] The effect of annealing of Pt surface at high temperature under vacuum and at partial pressures of N_2, O_2, and their mixture over the surface modification and the interfacial diffusion has been studied extensively by Moret *et al.*[20] The various mechanisms through which the surface roughening and the surface modifications take place have been studied extensively both by experiments and through theoretical calculations.[21,22] Hence, the modification of the platinum surface during the processing plays a crucial role in the phase formation of thin films.[18] In this work we have addressed the problem of phase formation of PMNPT over platinum substrates and the role of templates over the phase formation, micro structural evolution, and polarization behavior. The influence of surface modifications of the bare platinum under the present processing conditions used to fabricate PMNPT was studied. An intermediate roughening mechanism was observed under processing conditions. Further, the answers to the obvious questions such as: (i) What is the role of LSCO over the microstructural evolution of PMNPT? (ii) What is the minimum thickness of LSCO required for phase formation of PMNPT? (iii) What is its role over the phase formation? The size of the template layer and its effect over the polarization behavior of PMNPT of constant thickness are discussed in the present work.

II. EXPERIMENTAL

A phase pure homogeneous and high dense LSCO and PMNPT ceramic pellets of 12 mm of diameter and 5 mm thickness were prepared through a conventional solid state reaction and coloumbite process, respectively.[23] Thin films of LSCO and PMNPT were fabricated using a KrF pulsed excimer laser of 248 nm wavelength (lambda physik) over a commercially available platinized silicon substrate ($Pt/TiO_2/SiO_2/Si$). The pulsed laser ablation gives an opportunity to stop the deposition at the initial stages close to the formation of nucleation by firing a few laser pulses over the ceramic targets. The platinum films (~120 nm) are actually deposited over a (~50 nm) TiO_2 buffer layer sputtered over the native SiO_2 layer of silicon wafers and available commercially (Inostek corporation). The films were deposited at a substrate temperature of about 650 °C and 100 mTorr of oxygen ambient during the growth and laser was fired at energy of 150 mJ with an energy fluence of 2.5 J/cm^2. The phase purity, the microstructure and the electrical behavior of the PMNPT thin films fabricated at these conditions are studied in detail and have been reported earlier.[24] The surface modifications of the platinum substrates upon heating to high temperatures have been studied in detail by various researchers and are available in literature.[19–22] Hence, the modification of the platinum substrate surface prior to the deposition was studied in the deposition chamber and in exactly the same deposition conditions to mimic the surface as seen by the ablated species. Various films with a varying LSCO thickness (1–200 nm) and a constant PMNPT thickness (400 nm) were deposited. The LSCO thickness was even limited to a few unit cell thicknesses (1 nm) or, in other words, the deposition was stopped such that the LSCO layer is just allowed to have a stable nucleus over the platinum surface at random nucleation sites, which was achieved by firing only a few laser pulses over the LSCO target material. The surface modification of the platinum substrate and the random nucleation of both LSCO and PMNPT and the evolution of microstructure of the thin films were analyzed using an atomic force microscope (AFM). Surface roughness observed from the AFM studies was further analyzed using ellipsometric studies. Spectroscopic ellipsometry measurements of platinized substrates were carried out at room temperature in the photon energy range of 0.75–4.0 eV using a computer controlled variable angle of incidence spectroscopic ellipsometer (SENTECH 850, SETTECH Instruments) with a rotating polarizer rotating analyzer. The measurements were done in air at a 70° angle of incidence. The standard ellipsometric parameters Ψ and Δ were measured, which are related to the ratio ρ of the Fresenal coefficients, r_s and r_p for s and p polarizations, respectively,[25]

$$\rho \equiv \frac{r_p}{r_s} = \tan \Psi \exp(i\Delta), \tag{1}$$

where Ψ and Δ are the ellipsometric parameters. The ellipsometric data were analyzed by using the SpectraRay2-5656b software package (SETTECH Instruments). A program based on the least square regression was used to obtain the unknown fitting parameters by varying the fitting parameters to minimize the difference between the measured and calculated Ψ and Δ values. The formula given below was used to calculate the figure of merit (FOM), which was minimized for a best fit

$$\mathrm{FOM} = \frac{1}{N}\sqrt{\sum_{i=1}^{N}\left\{(\Psi_i^m - \Psi_i^{\mathrm{th}})^2 + (\Delta_i^m - \Delta_i^{\mathrm{th}})^2\right\}}. \tag{2}$$

Where N is the total no of parameters fitted and i is the summation index. The calculated data Ψ_i^{th} and Δ_i^{th} are generated by using the appropriate models.[26] The crystallinity of the films was studied using a powder x-ray diffractometer (Philips, Cu $K\alpha$, $\lambda = 1.541$ Å). The microstructure and the phase purity was studied in a cross sectional view of the fabricated thin film using a transmission electron microscope (TEM). The basic role of the template layer over the phase formation was further analyzed using x-ray photoelectron spectroscopic (XPS) studies. The binding energies of the Pb, Nb, and Ti were analyzed using Mg $K\alpha$ radiation and the binding energy of the Mg was analyzed using an Al $K\alpha$ radiation as a probe over the PMNPT layer with and without the template layer over the Pt (111) surface. The polarization behavior of the PMNPT layer of constant thickness for various thicknesses of LSCO was studied using a radiant technology high precision loop tester.

III. RESULTS AND DISCUSSION

A. Surface studies on pristine substrates

Figure 1(a) shows the surface of a pristine as a received platinized silicon wafer. The AFM micrograph shows smeared out grains close to spherical in the range of 20–40 nm of grain size. The morphology of this pristine platinum surface was consistent with most of the as received wafers which were randomly selected and examined. Platinum coated over the TiO_2 on silicon wafers are well-known to undergo various surface modifications under the processing conditions prior to the deposition of the material of interest, due to strain relaxation and gives rise to the formation of hillocks, pits, etc. and effectively roughening the surface.[19–22] Figures 1(b) and 1(c) show the surface of the substrate which has been heated to the deposition temperature (650 °C) under vacuum. The evolution of the pyramid shaped hillocks is clear from the AFM study which has been observed by various researchers and reported earlier.[19,20] Evolution and growth of these pyramidlike structures over a platinum (111) surface has been studied both theoretically and experimentally and is due to the surface diffusion of the platinum atoms.[21,22] The hillocks were observed to be of 80–120 nm height and a size of 5–40 nm in the lateral directions, effectively giving rise to an average root mean squared (rms) roughness of about 25 nm over an area of

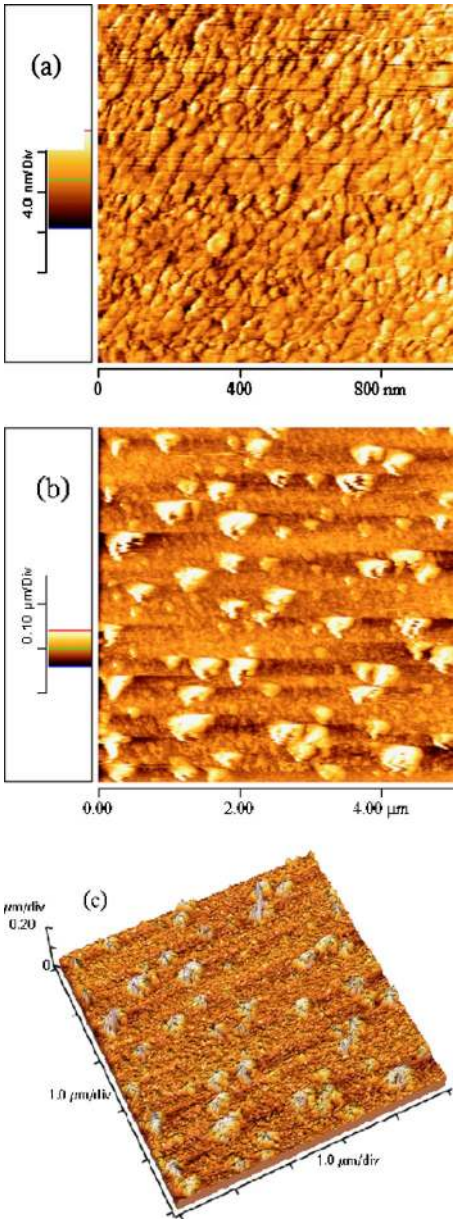

FIG. 1. (a) (Color online) AFM image of a pristine Pt substrate surface; (b) AFM image of a heat treated Pt substrate surface; (c) 3D image of a heat treated Pt substrate surface.

20 $\mu \times 20$ μ scan. Upon heating the platinum substrates to 650 °C, the appearance of these hillocks and the dimensions are consistent with the earlier studies available in the literature.[19,20]

A modulated wave pattern over the surface of the platinum was observed as an associative roughening mechanism along with the formation of these hillocks. As explained earlier, the platinum substrates used are actually a combination of multilayers and not a single platinum film over the silicon wafer. The presence of the deposition strain over the platinum surface, as well as at the interfaces present, leaves the platinum surface under a permanent planar strain. A stressed body is known to become unstable against undulations or spontaneous formation of stressed domains. A planar stressed surface of a multilayer being unstable against undulation is known as the Asaro-Tiller-Grienfeld (ATG) instability.[27,28]

As an effect of stress relaxation, the planar surface modifies to a periodic one-dimensional undulation in the form of $z(x)=h\cos(\omega x)$, where ω is the wave vector of the pattern and h is the amplitude of the stress wave on the surface. The amplitude and periodicity are highly dependent over the planar stress of the multilayers and the thickness of the layers. In our case the periodicity and the amplitude of the pattern varies spatially which could be due to the uneven stress distribution over the platinum surface. The crests and the valleys could have either tensile or compressive stress depending on the average planar stress levels.[29] The ripple pattern observed over the heat treated platinum surfaces as shown in Fig. 1(b) could be due to the ATG instability.

The undulation over the surface gives rise to a change in free energy and a distribution of stress over the modulated pattern. The free energy variation due to the ATG instability contains two terms

$$\Delta F = \Delta F_1 + \Delta F_2. \tag{3}$$

Where the first term is due to the capillary energy change due to the surface area increase and is given by

$$\Delta F_1 = \frac{\gamma}{4} h^2 \omega^2. \tag{4}$$

Where γ is the surface energy and the above equation is valid for very small h/λ and small slopes.[30] The second term ΔF_2 is the elastic energy change per unit area induced by the undulation. In a simplified calculation the ΔF_2 has been calculated as given below

$$\Delta F_2 = -4(1-\nu^2)\sigma^2 h^2 \omega / E. \tag{5}$$

Where υ is the Poisson's ratio, σ is the planar stress, and E is the Young's modulus. The resultant change in free energy is given by the combination of both the surface energy change and the change in the elastic energy. The elastic energy drops when an undulation develops on an in-plane stressed solid irrespective of the solid is under tensile or compressive stress. The surface energy does not follow the same as the elastic energy; hence, the modification of the surface into a wavy pattern alone does not minimize the surface energy.[29] Hence, the hillocks are observed to appear only at the valleys which could be due to the high concentration of compressive stress at the valleys than that of the crests. The modulation of the surface into a wave pattern due to stress relaxation is followed by the formation of the hillocks over the platinum surfaces. The amplitude and the periodicity of the undulation on the surface of platinum are highly sensitive to the dimensions of the individual layers present in the substrate. Analyzing the role of dimensions of individual layers over the modifications of the substrate surface is beyond the scope of this article. Later the substrates were heated in an oxygen ambient of 100 mTorr to mimic the exact deposition conditions. Smearing of the edges of the hillocks was observed and the sharp edges transforms to curved edges as reported in the literature.[20] The detachment of Pt atoms at the tip and their surface diffusion and the diffusion along the step edges are the two favorable mechanisms that has been studied extensively both by experiments and theoretical calculations and is responsible for the smearing of the Pt hillocks when heated under oxygen pressures.[20] The average roughness of the heat treated Pt surface was found to be around 18 ± 2 nm and was further confirmed from the ellipsometry studies.

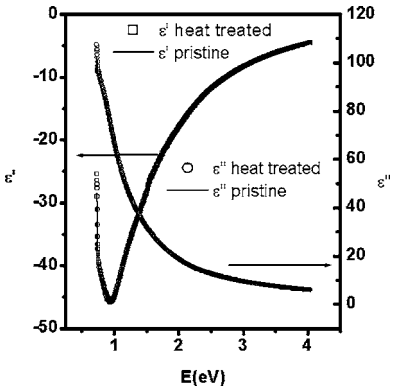

FIG. 2. Experimentally observed and fitted complex dielectric function for Pt surfaces.

The optical constants of platinum were determined from the ellipsometric measurements carried over the platinum substrates. The dielectric function of the platinum layer was obtained by the evaluation of a model with a rough surface. The roughness was modeled with the Bruggman effective medium approximation[26] assuming voids and dense Pt as constituents. The thickness d_{rough}, and fraction of inclusion f_r of the rough Pt layer, the thickness of the dense Pt layer, and the overall complex dielectric function $\varepsilon=\varepsilon_1+i\varepsilon_2$ of Pt were the fitting parameters in this study.

Figure 2 shows the complex dielectric function $\varepsilon=\varepsilon_1+i\varepsilon_2$ of Pt obtained from the pristine and heat treated Pt surfaces. The optical constants were determined by numerical inversion of the measured Ψ and Δ with the correction for the surface roughness. The values are in good agreement with the optical data of Pt in the literature.[31] As it is clear from Fig. 2, the dielectric function of platinum displays a Drude behavior, i.e., ε_1 increases with increasing photon energy while ε_2 decreases with increasing photon energy. But the deviation from the free electron behavior is seen at a low photon energy. This strong absorption in Pt around 1 eV can be accounted for the interband transition occurring between the p-like L_6^- band and the d-like $L_4^+L_5^+$ band above E_F and nearby regions of the k space.[31] This is the likely cause for the minimum of ε_1 at around 1 eV, but some authors such as Jungk *et al.*[32] points out that a similar effect can be caused by impurities or surface roughness within effective medium theories. In our experiment, we took two samples with different surface roughness, and found that the minimum in ε_1 occurs at same energy, therefore, this minimum might be due to the interband transitions. For each sample, the complex dielectric function (ε), the thickness d_{Pt}, and porosity f_v were obtained from the ellipsometric measurements in the air. For the two samples, the porosity increases from 0.02 for the pristine surface to 0.33 for the heat treated surface, respectively. The values of the roughness were in close agreement with the atomic force microscopy results.

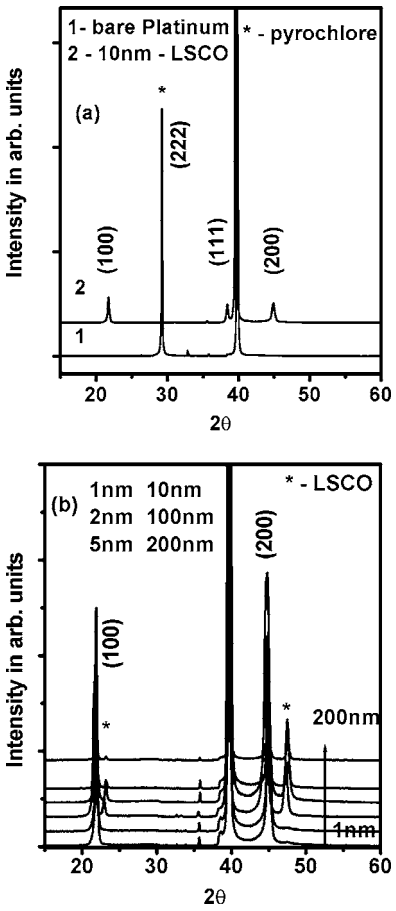

FIG. 3. (a) XRD pattern of a PMNPT thin film with and without a template layer. (b) XRD pattern of a PMNPT thin film over various LSCO thicknesses.

B. Structural and micro structural evolution

1. X-ray diffraction

Figure 3(a) shows the XRD pattern of the PMNPT thin films deposited over a bare platinum surface and over a thin (~10 nm) template layer of LSCO on a platinum surface. The pattern clearly shows the formation of a pyrochlore phase when PMNPT is deposited over the bare platinum surface. On deposition of a LSCO template layer of a thickness as low as 2 nm it gives rise to a pyrochlore free phase pure PMNPT perovskite phase. The need of a template layer to obtain a phase pure PMNPT thin film over platinum surfaces is unavoidable. The minimum thickness of LSCO to obtain a phase pure PMNPT thin film was further analyzed and was found that even the small stable nuclei formed from only ten laser pulses fired at the target is sufficient to obtain a phase pure PMNPT thin film of required thickness. Figure 3(b) shows the XRD pattern of PMNPT thin films of constant thickness (400 nm) deposited over various thicknesses of the LSCO layer. The thickness of the LSCO layer was optimized to vary with number of pulses fired by the laser while keeping the other processing conditions unchanged. Figure 3(b) includes the LSCO layer deposited from 10 laser pulses to 15 min of deposition of the LSCO layer. The optimization of the thickness with respect to the deposition time was carried out using a cross sectional scanning electron microscope and through depth profiling using a secondary ion mass spectrometer (cameca 4*f*). Hence, a pyrochlore free PMNPT perovskite phase can be obtained from even a few unit cell thicknesses of LSCO.

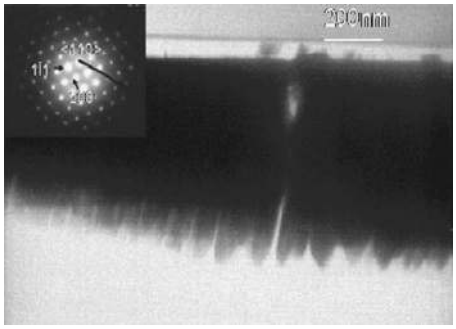

FIG. 4. Cross sectional TEM image of a PMNPT thin film and SAED pattern of the same.

2. TEM studies

The phase purity and the morphology of the template grown film was further analyzed through a transmission electron microscope. The thin film fabricated was thin down perpendicular to the growth direction such that the electron beam travels parallel to the film substrate interface and gives a cross sectional view of the growth structure. Figure 4 shows a clear columnar growth of grains with a column width of around 30–60 nm and the length of a column being the thickness (0.4 μm) of the film itself. The inset of Fig. 4 shows the selected area electron diffraction (SAED) pattern of a single grain and confirms the absence of any secondary phase present in the film.

3. AFM studies

The ultrathin LSCO deposited from very few (10) laser pulses are quite insufficient to form a continuous film or to completely cover the Pt surface. Hence, the role of LSCO in the nucleation of PMNPT and the evolution of microstructure was further analyzed through AFM studies. Figures 5(a) and 5(b) shows the surface morphology of the modified platinum surface on which LSCO was deposited with only 20 and 30 laser pulses fired at the LSCO target, respectively. Figures 5(c) and 5(d) shows the three-dimensional image of the substrate surface on which, 20 and 30 shots of LSCO was fired. The figures clearly show a random site island growth nucleation has taken place or alternatively known as Volmer-Weber type of growth.[33] As explained earlier, the hillocks observed over the heated platinum surfaces plays a crucial role in the nucleation of the thin film. Though the nucleation picture gives an impression of random site selection, the actual sites that are energetically favorable for the nucleation are the tip of the hillocks. The surface morphology clearly shows the preferential site for the nucleation of the LSCO layer is the tip of hillocks observed over the platinum surfaces. Figures 5(c) and 5(d) clearly shows that the further growth of the layer is continued along the direction of the tips of the hillocks and the next nuclei grows adjacent to the previous stable nuclei. It is also evident from the morphology that the growth begins only from the tips of the hillocks that are present in the valleys of the surface. As explained

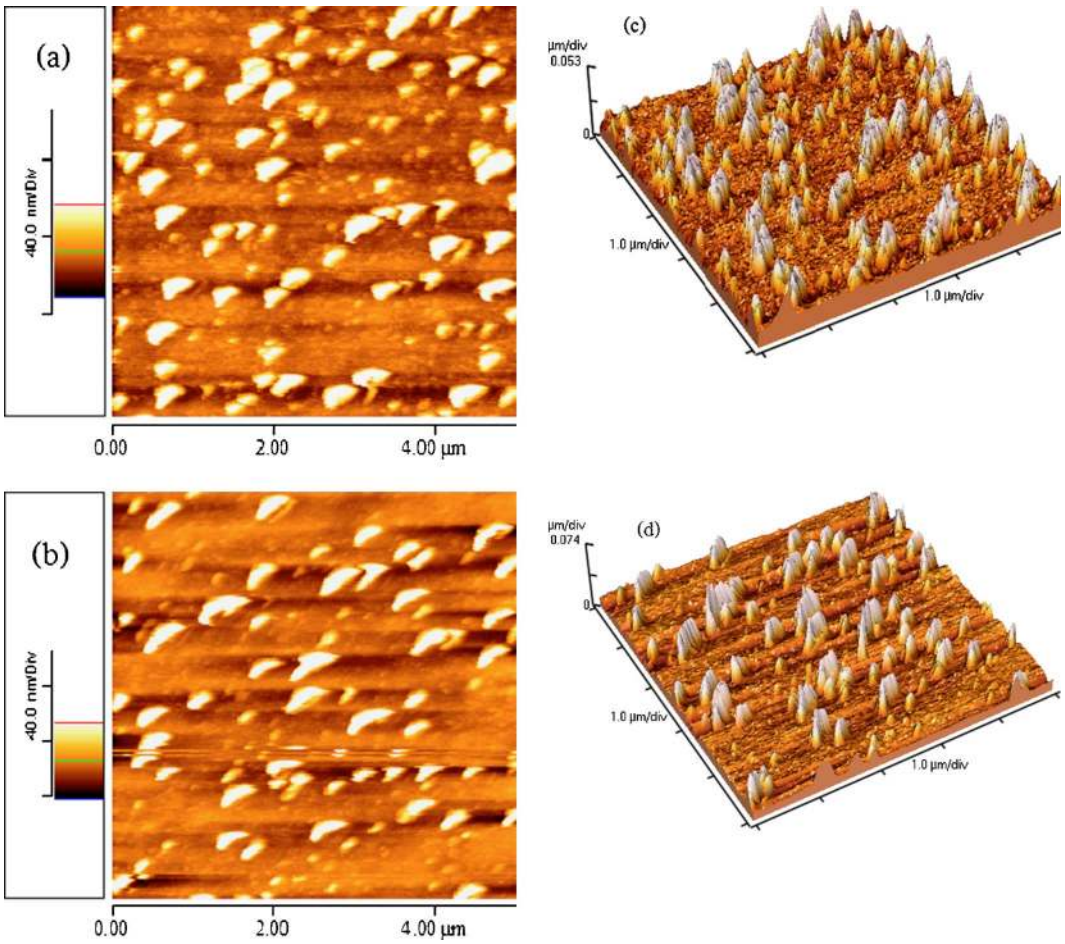

FIG. 5. (a) (Color online) AFM image of LSCO deposited from 20 laser pulses; (b) AFM image of LSCO deposited from 30 laser pulses; (c) 3D image of LSCO deposited from 20 laser pulses; (d) 3D image of LSCO deposited from 30 laser pulses.

earlier, the tips of the Pt hillocks are at higher energy and hence the growth of the LSCO layer at the tips give a favorable change of free energy of the system effectively stabilizing the embryo as a stable nuclei.[33] To understand the growth morphology a deposition with 20 shots of the LSCO layer was done over which, 70 shots of laser pulses fired on PMNPT was deposited and the surface morphology is shown in Figs. 6(a) and 6(b). Figures 6(a) and 6(b) clearly show that the growth of the islands continues along the direction of the tips and introduces a connectivity across the crests and effectively gives rise to an oriented growth connecting the hillocks. Figure 6(b) shows the line profile at three different regions along the x direction of the surface of PMNPT films grown from 70 shots of laser pulses deposited over 20 shots of laser pulses over LSCO. The line profile clearly shows the wavy pattern of the surface at three different regions. The platinum surface between the hillocks remains uncovered by the growth. Further increase in the deposition time or increase in the number of laser pulses gives rise to a growth in the lateral direction or a coalescence of the nuclei in the two-dimensional plane and effectively covering the uncovered areas of the platinum surface.[33] The minimum thickness required to have a uniform film was found to be around 40 −50 nm. A film grown for about 40 nm thick is known to be uniform over the surface with an rms roughness less than 2 nm. Thus the growth morphology observed at various stages of the thin film growth clearly shows that the optimized growth parameters gives rise to a columnar growth of islands and finally coalesce in the lateral direction to give a uniform dense film. Figure 6(c) shows the surface morphology of a PMNPT film coated over bare platinum surface without the LSCO template layer. The morphology clearly shows that a cubic pyrochlore phase emerges and destabilizes the perovskite phase of PMNPT. The pyrochlore phase also had a randomly nucleated island growth alternatively known as the Volmer-Weber growth.[33] The role of the template layer over the nucleation and the evolution of the microstructure have been understood from the above discussions, whereas the role of the template layer over the phase formation remains ambiguous. Hence, the binding energies of the individual species were studied further by x-ray photoelectron spectroscopy (XPS).

C. XPS studies

Figures 7(a) and 7(b) show the core level XPS spectrum of Pb and Nb, respectively, with and without a template layer. The core level spectra of Ti $2p$ and O $1s$ exhibited a least variation with and without a template layer. Figure 7(a) shows the Pb spectra for the films deposited with and without the template layer. The spin-orbit doublets of the $4f$ orbital of Pb is clearly seen for the film deposited with the

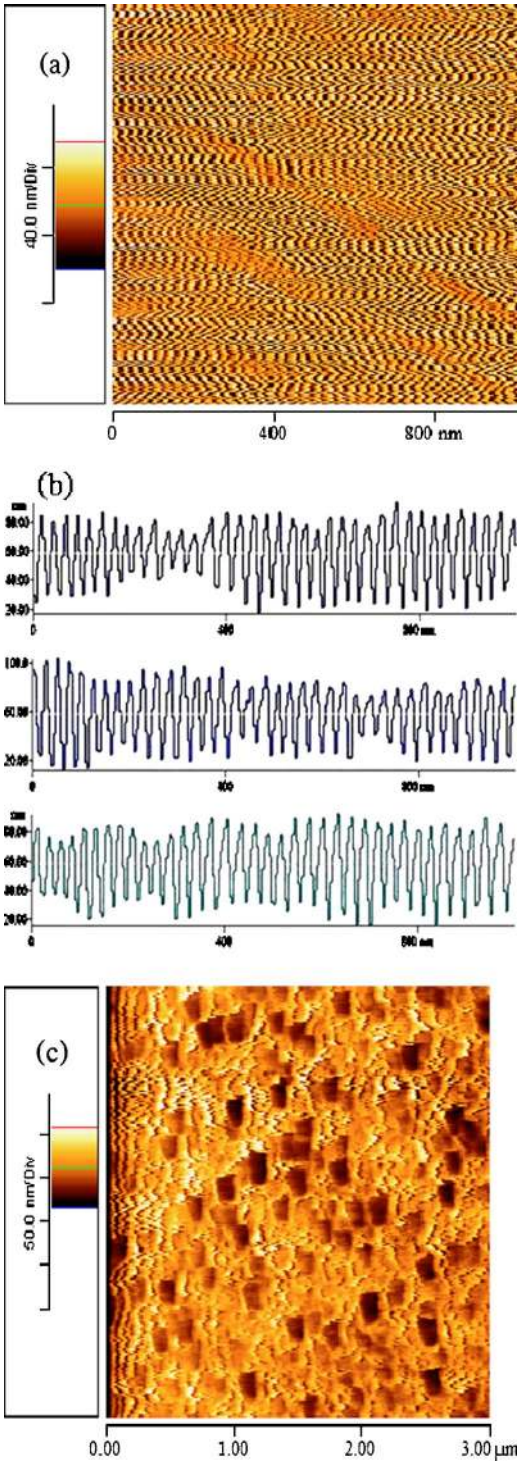

FIG. 6. (a) (Color online) AFM image of 20 laser pulses of LSCO followed by 70 pulses of PMNPT; (b) line profile taken over the surface of 20 laser pulses of LSCO followed by 70 pulses of PMNPT; (c) AFM image of a PMNPT film deposited over bare Pt surface.

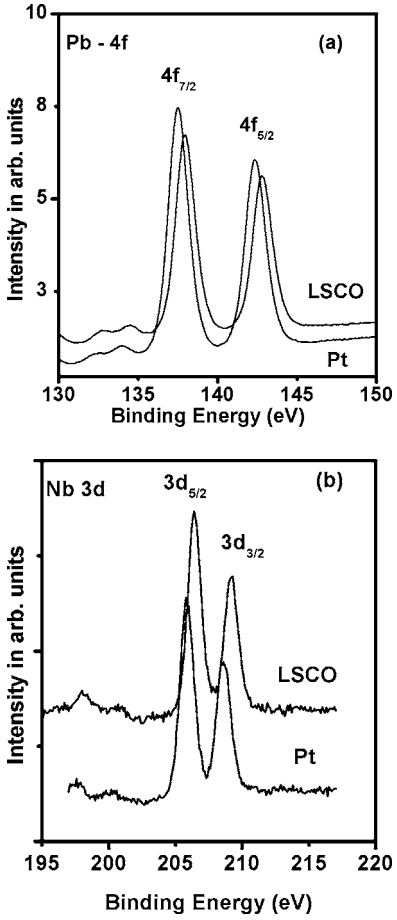

FIG. 7. (a) XPS spectrum of Pb 4*f* for PMNPT film deposited over LSCO and Pt; (b) XPS spectrum of Nb 3*d* for PMNPT film deposited over LSCO and Pt.

template layer and the binding energies are about 138 and 142.8eV corresponding to the Pb $4f_{7/2}$ and Pb $4f_{5/2}$, respectively. The binding energy difference between the spin orbit doublets were found to be around 4.8 eV with a chemical shift of around +1.1 from the elemental binding energy of Pb (136.9 eV) and the observed binding energies coincides well with the earlier studies made on PMNPT single crystals and corresponds to the Pb^{2+} state. The observed single spin-orbit doublet for the films deposited over the template confirms the absence of mixed oxidation states and the spectrum observed could be attributed to the lattice Pb state.[34] The Pb 4*f* spectrum of the film deposited over the bare platinum surfaces exhibited a shift of 0.5 eV toward the lower binding energies and close to the catalog value of pure Pb (136.9 eV) which could be due to the partial reduction of Pb^{2+} to a metallic Pb^0 surface state. Figure 7(b) shows the core level energy spectrum of Nb corresponding to the 3*d* orbital. The spectrum observed for the film deposited over template clearly shows the spin-orbit doublets of $3d_{5/2}$(206.4 eV) and $3d_{3/2}$(209.3 eV) lines, and the observation of single doublet clearly shows the absence of mixed oxidation states of Nb. The binding energy difference between the spin-orbit doublets were found to be around 2.9 eV with a chemical shift of around +4.0 from the elemental binding energy of Nb (202.4 eV), and the observed binding energies coincides well with the earlier studies made on PMNPT single crystals and corresponds to the Nb^{5+} state.[34] Hence, the spectrum of Nb observed for the PMNPT films deposited over the template layers clearly shows the single oxidation state of Nb and corresponds to the Nb^{5+} sublattice in the perovskite phase of PMNPT. The spectrum of Nb observed for PMNPT films over bare platinum shows a clear shift of 0.7 eV toward the lower energies which could be attributed to the reduction of Nb^{5+} to the Nb^{4+} state. The reduction of Nb^{5+} to its lower

oxidation states has been observed and confirmed by various irradiation studies in which the Nb_2O_5 is subjected to electron irradiation and with respect to irradiation time, the Nb_2O_5 is driven to lower oxides.[35,36] Hence, this possible reduction of Nb^{5+} to Nb^{4+} can give rise to a charge imbalance to the structure and, hence, the system is driven from an unstable perovskite phase to a stable pyrochlore phase. As explained earlier the nucleation starts at the tip of the hillocks observed over platinum surfaces which are known as the high energy points of the hillocks.[21,22] These high energy tips could possibly drive the Nb to its lower oxidation states or to the formation of any lower oxides of niobium at the initial stage of the growth and effectively destabilizing the perovskite phase of PMNPT in which the charge state of Nb is more crucial for the stability and charge balance as explained earlier.[13,14] The platinum hillocks effectively drives Nb and Pb effectively to a mixed state and hence a slight shift observed in the Pb spectrum which was absent in the Pb spectrum corresponding to the sample in which Nb was observed to be in its highest oxidation state. Thus, the high energy tips of the platinum surfaces affects the initial growth of Nb and Pb and hence giving rise to a more stable pyrochlore phase. The XPS analysis was completed at the films that were grown from few laser pulses, whereas, it could be more useful and confirmative if the analysis of the growth is done at the cross section of the interface at the initial stages of the growth, which was limited currently due to experimental limitations. When the LSCO template is used the nucleation sites of the LSCO is chemically different from that of the Pt surfaces and, hence, the ablated species from PMNPT bonds with the LSCO nuclei at the tips of the hillocks, which stabilizes the perovskite phase of PMNPT. Nevertheless, extensive XPS studies and simulation of the same at the Pt-LSCO interface, Pt-pyrochlore interface, and LSCO-PMNPT interface on the cross sectional view of the sample could throw light on a conclusive chemical role of LSCO on the perovskite phase formation of PMNPT. Apart from the fundamental quest of phase formation on Pt substrates, the formation of the pyrochlore phase at the electrode and the bulk, which is attributed to the degradation of the functional PMNPT material, could be understood.

D. Polarization hysteresis

The variation of the remnant polarization (P_r) and the polarization behavior of the PMNPT thin films for various template layer thicknesses and constant PMNPT thicknesses were studied as a measure of illustrating the effect of the template layer. Figure 8(a) shows the room temperature polarization hysteresis behavior of a PMNPT film with a thickness of 400 nm for various thicknesses of the LSCO layer. The nano polar regions present in the PMNPT thin films acts as nano domains equivalent to the domains observed in normal ferroelectric systems. Under the electric field the nano domains orient and align themselves along the field direction which gives rise to saturation at a higher electric field.[2] The field induced long range interaction and the longer relaxation times of the relaxor FE gives rise to a remnant polarization and a polarization behavior similar to normal FE. Figure 8(b) shows the variation of P_r with the thickness of the LSCO template layer. The PMNPT thin films with a thickness of 400 nm and a different LSCO layer thickness exhibited a least variation over the polarization behavior. They exhibited a slim loop behavior, characteristic of a ferroelectric relaxor thin film with an average remnant polarization of $\sim 4\ \mu C/cm^2$ irrespective of the thickness of the LSCO template layer. Figure 8(c) shows a perfect linear dielectric behavior of a pyrochlore phase formed when PMNPT deposited over a bare platinum substrate.

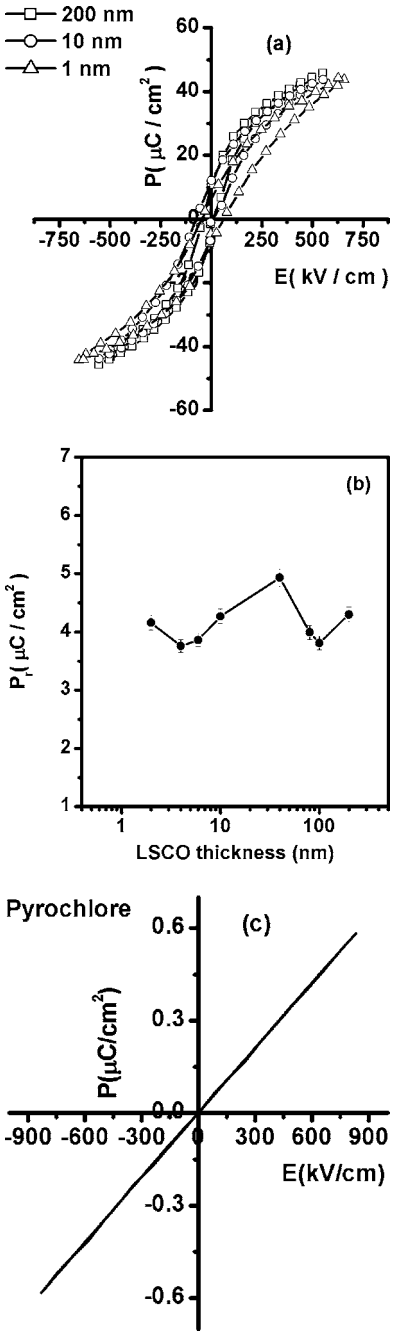

FIG. 8. (a) Polarization hysteresis of a PMNPT thin film for different LSCO thicknesses; (b) variation of remnant polarization with an LSCO thickness; (c) P-E characteristics of a pyrochlore phase of PMNPT.

IV. CONCLUSIONS

In summary, the phase formation of PMNPT over platinum substrates with and without a template layer was ana-

lyzed and the steps involved in the evolution of roughness of the platinum surface were studied using AFM and ellipsometry studies. Evolution of microstructure of PMNPT thin films was studied and was confirmed by AFM and TEM studies. The role of the template over the chemical state of the system was analyzed using x-ray photoelectron spectroscopy studies. The formation of hillocks over platinum substrates is known and studied extensively over decades, whereas depending on the platinum layer thickness and the TiO_2 layer used for adhesion of Pt over SiO_2 the formation of hillocks is associated with a strain wave pattern due to the ATG instability observed in a multilayer under planar stress. The troughs present in the surface due to the undulations are known to be under high compressive stress and hence the hillocks are observed to originate from the troughs of these undulations. The nucleation of PMNPT, as well as LSCO, was observed to form at the tip of the hillocks and the second nucleus forms adjacent to the previous one along the direction of the tip of the hillock. The sequence of this nucleation effectively gives rise to a wavy pattern of the film until the stable nucleus coalesces with each other in the lateral direction and effectively fills the surface of the substrate. The minimum thickness required to have complete coverage of the substrate area was found to be around 40 nm whereas, even few unit cells (1 nm) of LSCO is sufficient for the stabilization of the perovskite phase of PMNPT. The PMNPT thin films fabricated under the above explained processing conditions are known to have a columnar growth structure and was confirmed from a cross sectional TEM study and each column acted as a single crystal with a single phase and orientation as observed from SAED studies. Chemical states of the ablated species were analyzed using XPS measurements and the $3d$ core level spectrum of Nb and $4f$ of Pb were found to be in a single oxidation state of 5+ and 2+ corresponding to the lattice site of PMNPT when grown over the template. When deposited without a template as stated earlier, the nucleation starts at the tips of the hillocks which possibly give rise to a lower oxidation state of Nb 4+ and giving rise to a metallic Pb formation at the initial stage of growth. The charge state of Nb is more crucial in stabilizing the perovskite phase of PMNPT and, hence, the charge imbalance due to the reduction of Nb effectively destabilizes the perovskite phase and drives the system to a cubic pyrochlore phase. The polarization behavior of the PMNPT thin films was found to be insensitive to the thickness of the LSCO template layer. The remnant polarization of constant thickness of PMNPT grown over various thicknesses of LSCO remained almost constant with an average value of $\sim 4\ \mu C/cm^2$.

ACKNOWLEDGMENT

The authors acknowledge Ms. Neelam Kumari for her help in analyzing the ellipsometry data.

[1] G. A. Smolensky and A. I. Agranovskaya, Sov. Phys. Solid State **1**, 1429 (1959).
[2] L. E. Cross, Ferroelectrics **151**, 305 (1987).
[3] D. Viehland, S. Jang, L. E. Cross, and M. Wuttig, J. Appl. Phys. **68**, 2916 (1990).
[4] K. Uchino, *Piezoelectric Actuators and Ultrasonic Motors* (Kluwar Academic Publishers, Boston, 1996).
[5] N. Takesue, Y. Fujii, and H. You, Phys. Rev. B **64**, 184112 (2001).
[6] H. You and Q. M. Zhang, Phys. Rev. Lett. **79**, 3950 (1997).
[7] J. Chen, H. M. Chan, and M. P. Harmer, J. Am. Ceram. Soc. **72**, 593 (1989).
[8] Y. Yan, S. J. Pennycook, Z. Xu, and D. Viehland, Appl. Phys. Lett. **72**, 3145 (1998).
[9] S. Miao, J. Zhu, X. Zhang, and Z. Y. Cheng, Phys. Rev. B **65**, 052101 (2001).
[10] G. Xu, G. Shirane, J. R. D. Copley, and P. M. Gehring, Phys. Rev. B **69**, 064112 (2004).
[11] K. Hirota, Z. G. Ye, S. Wakimoto, P. M. Gehring, and G. Shirane, Phys. Rev. B **65**, 104105 (2002).
[12] R. Blinc, A. Gregorovic, B. Zalar, R. Pirc, V. V. Laguta, and M. D. Glinchuk, Phys. Rev. B **63**, 024104 (2000).
[13] E. Husson, M. Chubb, and A. Morell, Mater. Res. Bull. **23**, 357 (1988).
[14] V. Westphal, W. Kleeman, and M. Glinchuk, Phys. Rev. Lett. **68**, 847 (1992).
[15] T. R. Shrout and J. F. Fielding Jr., Proc.-IEEE Ultrason. Symp. **2**, 711 (1990).
[16] M. Dawber, K. M. Rabe, and J. F. Scott, Rev. Mod. Phys. **77**, 1083 (2005).
[17] A. Laha, S. Saha, and S. B. Krupanidhi, Thin Solid Films **424**, 274 (2003).
[18] J. Guo, H. L. M. Chang, and D. J. Lam, Appl. Phys. Lett. **61**, 3116 (1992).
[19] G. R. Fox, S. Troilier-Mckinstry, S. B. Krupanidhi, and L. M. Cascas, J. Mater. Res. **10**, 1508 (1995).
[20] M. P. Moret, M. A. C. Devillers, F. D. Tichelaar, E. Aret, P. R. Hageman, and P. K. Larsen, Thin Solid Films **434**, 283 (2003).
[21] P. J. Feibelman, Phys. Rev. B **60**, 4972 (1999).
[22] T. Michely *et al.*, Phys. Rev. Lett. **86**, 2589 (2001).
[23] S. Swartz and T. R. Shrout, Mater. Res. Bull. **17**, 1245 (1982).
[24] A. Laha, S. Battacharya, and S. B. Krupanidhi, Mater. Sci. Eng. B **106**, 111 (2004).
[25] R. M. A. Azzam and N. M. Bashara, *Ellipsometry and Polarized Light* (North-Holland, Amsterdam, 1977).
[26] D. E. Aspnes, J. B. Theeten, and F. Hottier, Phys. Rev. B **20**, 3292 (1979).
[27] R. J. Asaro and W. A. Tiller, Metall. Trans. **3**, 1789 (1972).
[28] M. A. Grinfeld, J. Intell. Mater. Syst. Struct. **4**, 76 (1993).
[29] *Stress and Strain in Epitaxy: Theoretical Concepts Measurements and Applications*, edited by M. Hanbucken and J.-P. Deville (Springer, New York, 2001).
[30] H. Gao, J. Mech. Phys. Solids **39**, 443 (1991).
[31] J. H. Weaver, Phys. Rev. B **11**, 1416 (1975).
[32] G. Jungk, Thin Solid Films **234**, 428 (1993).
[33] M. Ohring, *The Materials Science of Thin Films* (Elsevier, New York, 1991).
[34] A. Kania, E. Talik, M. Kruzek, and A. Slodczyk, J. Phys. Condens. Matter **17**, 6737 (2005).
[35] M. Grundner and J. Halbritter, J. Appl. Phys. **51**, 397 (1980).
[36] E. E. Latta and M. Ronay, Phys. Rev. Lett. **53**(9), 948 (1984).